

Gas Permeation Properties of Hexafluoro Aromatic Polyimides

KENJI MATSUMOTO* and PING XU

Central Research Laboratory, Nitto Denko Corporation 1-1-2, Shimohozumi, Ibaraki, Osaka, 567, Japan

SYNOPSIS

Two hexafluoro-substituted aromatic polyimides, 6FDA-*p*-PDA and 6FDA-4,4'-ODA, were synthesized. The influence of some synthetic conditions on physical properties and gas permeabilities of the 6FDA polyimide membranes were studied. Gas permeabilities and permselectivities of six different gases for the homogeneous films have been determined at 15–35°C and at pressures up to 10 atm. 6FDA polyimide composite membranes with asymmetric structure were prepared by the solution-casting method. The membranes showed exceptionally high permeation fluxes and permselectivities. No capability deterioration of asymmetric membrane was observed during 19 days operation with pure gases. © 1993 John Wiley & Sons, Inc.

INTRODUCTION

In recent years, gas-separation systems using permselective polymer membranes have been applied for many industries, and many types of gas-separation membranes are now being developed. Especially, CO₂/CH₄ separation membrane is actively studied for the application of the refining of natural gas, fermentation gas, and plant exhaust gas. For CO₂/CH₄ separation, polyimides as gas-separation membrane material are well known because of their excellent thermal, chemical, and mechanical stability. Recently, it was reported that polyimides with 2,2-bis(3,4-decarboxyphenyl)hexafluoropropane dianhydride (6FDA) exhibit both a higher gas selectivity and permeability than do general polyimides and more common polymers.^{1,2} Therefore, a number of studies on the relationship between the chemical structure of the 6FDA polyimide and their gas permeation and separation properties have been done.^{3–11}

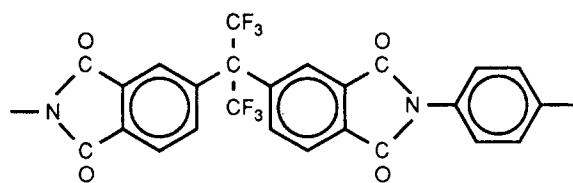
In the present work, the effect of the imidization method, monomer purity, and synthetic scale on the physical properties and gas permeability of 6FDA polyimide films was studied. Furthermore, gas per-

meabilities of two kinds of 6FDA polyimide films are compared with nonfluoropolyimide film. Finally, the preparation of asymmetric membranes that can be applicable for industrial use are reported. Capability change of the membrane with time is also reported.

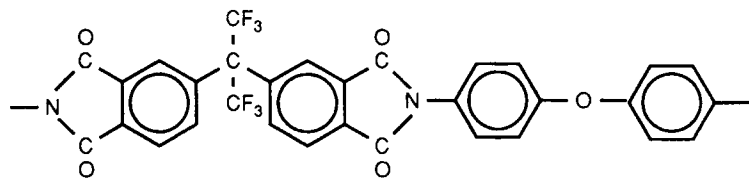
EXPERIMENTAL

The chemical structures of the polyimides used in this study are shown in Figure 1. 6FDA-4,4'-ODA steric structure simulated by a computer is given in Figure 2 as an example. Preparation of the process of 6FDA polyimides is shown in Figure 3. The polymerization reaction is performed by a two-step method. The first step comprises acylation of the diamine with 6FDA dianhydride in *N*-methyl-2-pyrrolidone (NMP) solvent to give the precursor polyamic acids. The second step is imidization of the polyamic acid to give rise to the 6FDA polyimide. The imidization is carried out in two different methods in this study. For chemical imidization, acetic anhydride is added to four times an equimolar amount of aromatic diamine as dehydrating agent and pyridine was added as catalyst. Polyamic acid solution was diluted to less than 10% to prevent gellation. For thermal imidization, *m*-xylene was added to five times an equimolar amount of aromatic

* To whom correspondence should be addressed.



6FDA-p-PDA



6FDA-4,4'-ODA

Figure 1 Chemical structure of polyimide used in this work.

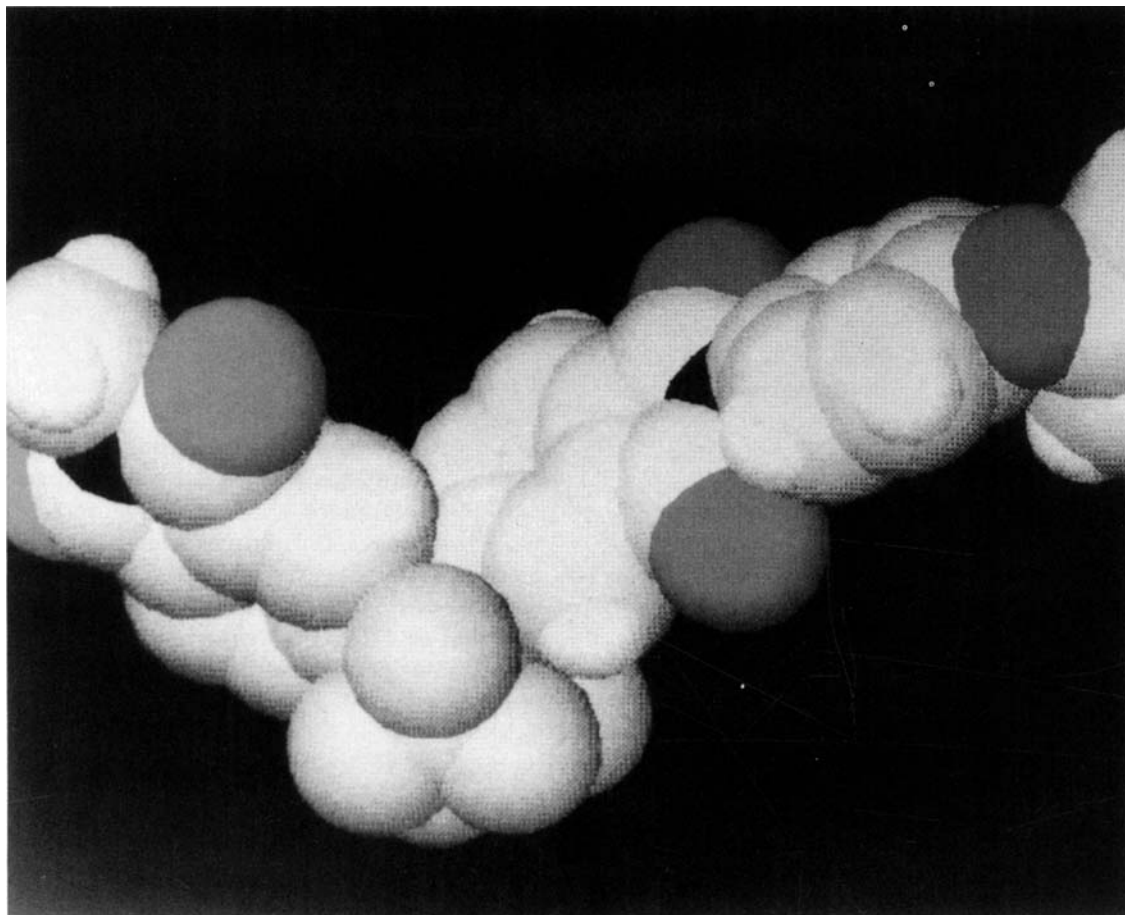


Figure 2 Steric structure of the 6FDA-4,4'-ODA simulated with computer calculation.

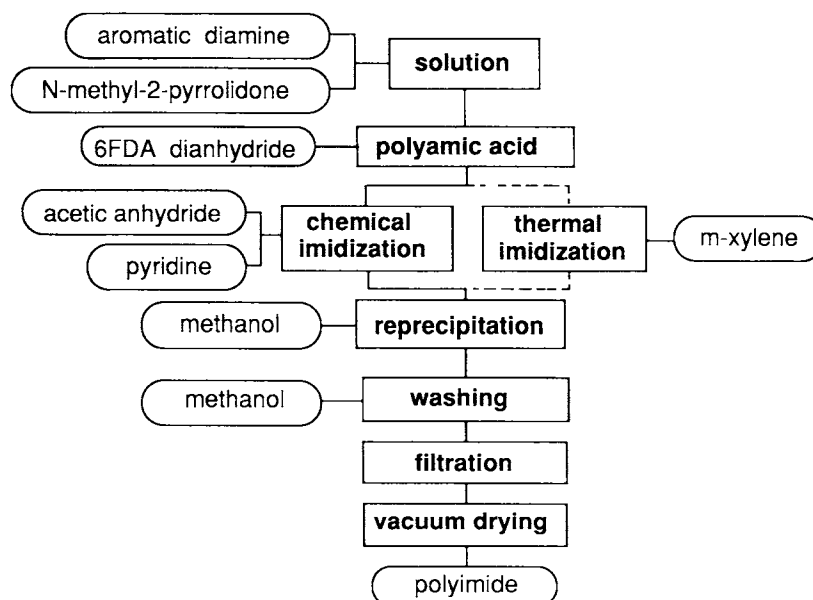


Figure 3 Preparation process of the 6FDA polyimide.

diamine as a low boiling azeotropic agent, and azeotropic distillation was performed at 150°C.

6FDA dianhydride monomers (Hoechst Chemikalien Co., 99% purity) were vacuum dried for 2 h at 180°C and then for 24 h at 40°C. NMP (Waco Co., 98% purity) was dehydrated using a molecular sieve and then was vacuum-distilled under a nitrogen atmosphere. Polymerization was carried out at room temperature under a nitrogen atmosphere.

The polyimides in this study were used in the form of homogeneous films and asymmetric membranes. The films were prepared by casting the solutions of 5–8% (weight) for 6FDA-4,4'-ODA and

15–18% for 6FDA-*p*-PDA in NMP on clean glass plates with an applicator. Solutions were filtered through a 2 μm filter prior to casting in order to remove any large particles or impurities. The resulting films were dried in an oven at 100°C and 150°C for 5 h, respectively, and at 250°C for 3 h. Final thicknesses of films were 15–35 μm.

The asymmetric membranes, having a thin skin layer and a thick porous matrix layer, were prepared by casting NMP solution of the 6FDA polyimide on polyester nonwoven cloth and then were solidified in ice water and dried in air.

The chemical structure of polymers synthesized

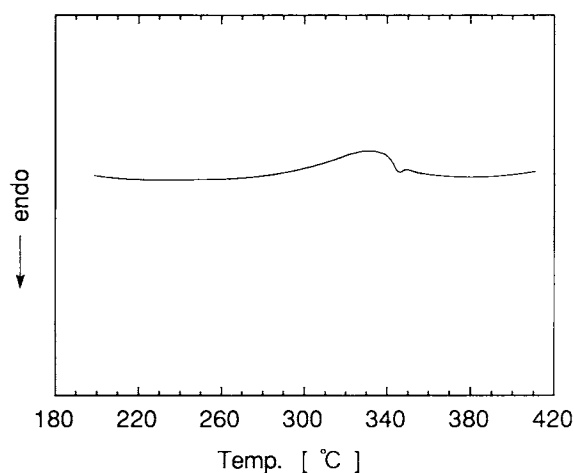


Figure 4 DSC thermogram of the 6FDA-*p*-PDA polyimide D film.

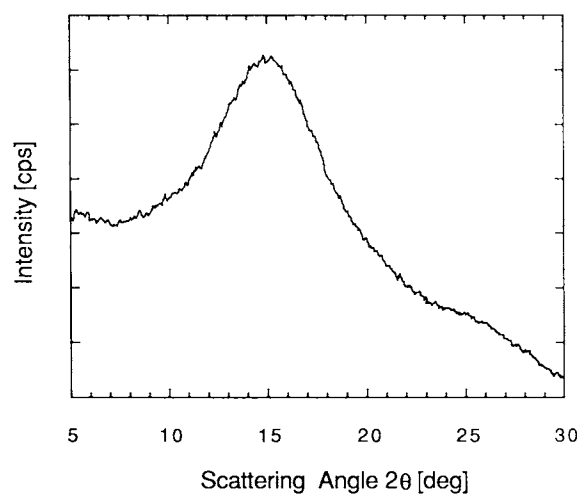


Figure 5 WAXD result of 6FDA-4,4'-ODA polyimide C film; CuKα radiation; λ = 1.54 Å.

Table I Physical Properties of the Polyimides Prepared in This Study

No.	Polymer	Imidization	Scale (mol)	M_n (-)	M_w (-)	η (dL/g)	ρ (g/cm ³)	T_g (°C)	" d " (Å)
A	6FDA-4,4'-ODA	Chemical	0.04	76,100	537,000	2.37	1.431	297.2	5.88
B	6FDA-4,4'-ODA	Chemical	0.30	36,000	150,000	2.05	1.429	296.8	5.94
C	6FDA-4,4'-ODA	Thermal	0.04	6,950	15,000	0.442	1.416	288	5.87
D	6FDA- <i>p</i> -PDA	Chemical	0.04	23,500	93,900	0.815	1.451	338	5.63
E	6FDA- <i>p</i> -PDA	Chemical	0.04	13,300	46,200	0.559	1.451	328	5.79

D: *p*-PDA is 99.95% purity; E: *p*-PDA is 97% purity.

was characterized by nuclear magnetic resonance (NMR). The weight-average molecular weight, M_w , and number-average molecular weight, M_n , were measured by gel permeation chromatography (GPC) performed on dilute solution of polyimides in NMP. Glass transition temperatures, T_g , of films were determined by differential scanning calorimetry (DSC). Average interchain distances " d "-spacing^{1,2} were obtained from wide-angle X-ray diffraction (WAXD) measurements of the films. The inherent viscosities η were obtained by measuring the viscosity of the polyimide solution at a concentration of 0.5 g/dL in NMP at 30°C. The densities, ρ , of films at 25°C were obtained by an accurate balance measuring the specific gravity of the films in air and in water by using following equation:

$$\rho = W_A(\rho_W - \rho_A)/(W_A - W_W) + \rho_A \quad (1)$$

where W_A and W_W are polymer weight in air and water, respectively, and ρ_W and ρ_A are polymer density in air and water, respectively.

Steady-state gas permeation measurements of polyimides were carried out by use of the pressure transform method at 15–35°C at pressures up to 10

atm. Permeation rates of hydrogen, carbon dioxide, oxygen, carbon monoxide, nitrogen, and methane in the homogeneous films and asymmetric membranes were determined using an Baratoron pressure transducer and digital equipment with a personal computer. The downstream pressure of the membrane was always 10 Torr or less.

RESULTS AND DISCUSSION

Typical results of the T_g of the 6FDA-*p*-PDA polyimide D film and " d "-spacing of the 6FDA-4,4'-ODA polyimide C film are shown in Figures 4 and 5, respectively. All physical properties obtained are summarized in Table I. To examine the influence of the imidization method and synthetic scale on the physical properties and gas permeabilities, 6FDA-4,4'-ODA were synthesized using the chemical imidization (polyimide A and B) and thermal imidization methods (polyimide C). Furthermore, for chemical imidization, two different synthetic scales were employed, i.e., the reaction quantity of polyimide B was 7.5 times larger than that of polyimide A.

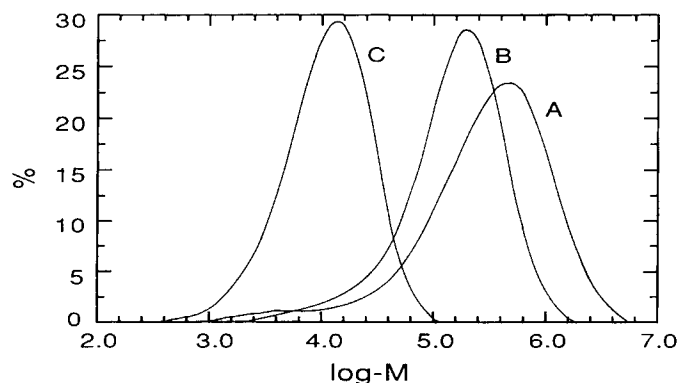


Figure 6 Molecular weight distribution curves of the 6FDA-4,4'-ODA polyimides by GPC analysis.

The chemical structure of 6FDA-4,4'-ODA for the three polyimides has been confirmed by ^{13}C -NMR analysis, and impurities were scarcely detected. Molecular weight distributions of the three types of 6FDA-4,4'-ODA polyimides measured by GPC are shown in Figure 6. There appeared big differences in molecular weight among the three types of polyimides, the polyimides with larger viscosity of the solution having higher molecular weight. M_n (or M_w) and η of polyimide A obtained by a small synthetic scale are larger than those of polyimide B obtained by a large scale due to the higher polymerization of small-scale polyimide, but there are no big differences in T_g and ρ . On the other hand, in the same synthetic scale, M_n (or M_w), η , ρ , and T_g of polyimide C obtained by thermal imidization are markedly lower than those of polyimides A and B obtained by chemical imidization.

To examine the effect of diamine purity on physical properties and gas permeability of 6FDA polyimide, polyimides D and E were synthesized using *para*-phenylenediamines (*p*-PDA) with 99.95% (purified) and 97% (commercial) purities, respectively, by the chemical imidization method. From Table I, it is clear that by increasing diamine purity from 97% to 99.95% M_n and η are increased 1.8 and 1.5 times, respectively; also, T_g is increased by 10°C .

The ideal separation factor $\alpha_{\text{CO}_2/\text{CH}_4}$ ($= P_{\text{CO}_2}/$

P_{CH_4}) as a function of CO_2 mean permeability coefficient P_{CO_2} are plotted in Figure 7 for the 6FDA polyimides obtained in the present work. As shown in Figure 7, P_{CO_2} and $\alpha_{\text{CO}_2/\text{CH}_4}$ of polyimides A and B synthesized by using chemical imidization are almost the same in spite of the difference in M_n (or M_w) and η due to a synthetic-scale difference. The result is consistent with fact that T_g and ρ of polyimides A and B are almost the same. On the other hand, P_{CO_2} and $\alpha_{\text{CO}_2/\text{CH}_4}$ of polyimide C synthesized by thermal imidization are clearly low compared with those of polyimides A and B.

For 6FDA-*p*-PDA polyimide, as shown in Figure 7 at the same temperature (25°C), polyimide D made of 99.95% purity diamine shows both higher selectivity and higher permeability than does polyimide E made of 97% purity commercial diamine. Generally, 6FDA-*p*-PDA shows better permeability and selectivity than does 6FDA-4,4'-ODA.

Data^{1,2} of a number of nonfluoro-PMDA polyimides and commercial polymers are also shown in Figure 7 for comparison. The gas mean permeability coefficients of 6FDA polyimides are largely increased as compared to PMDA polyimides and commercial polymers, while high permselectivity of 6FDA polyimides are retained. This result can be explained considering that the bulky $-\text{C}(\text{CF}_3)_2-$ group in the polymer backbone contributes to the increase in

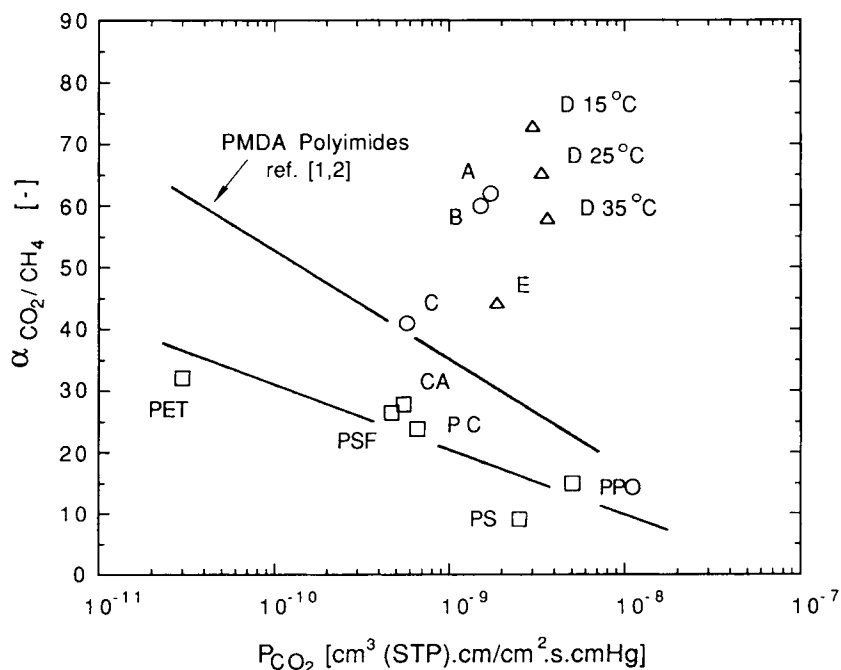


Figure 7 The relationship between ideal separation factor $\alpha_{\text{CO}_2/\text{CH}_4}$ and mean permeability coefficient P_{CO_2} for 6FDA polyimides.

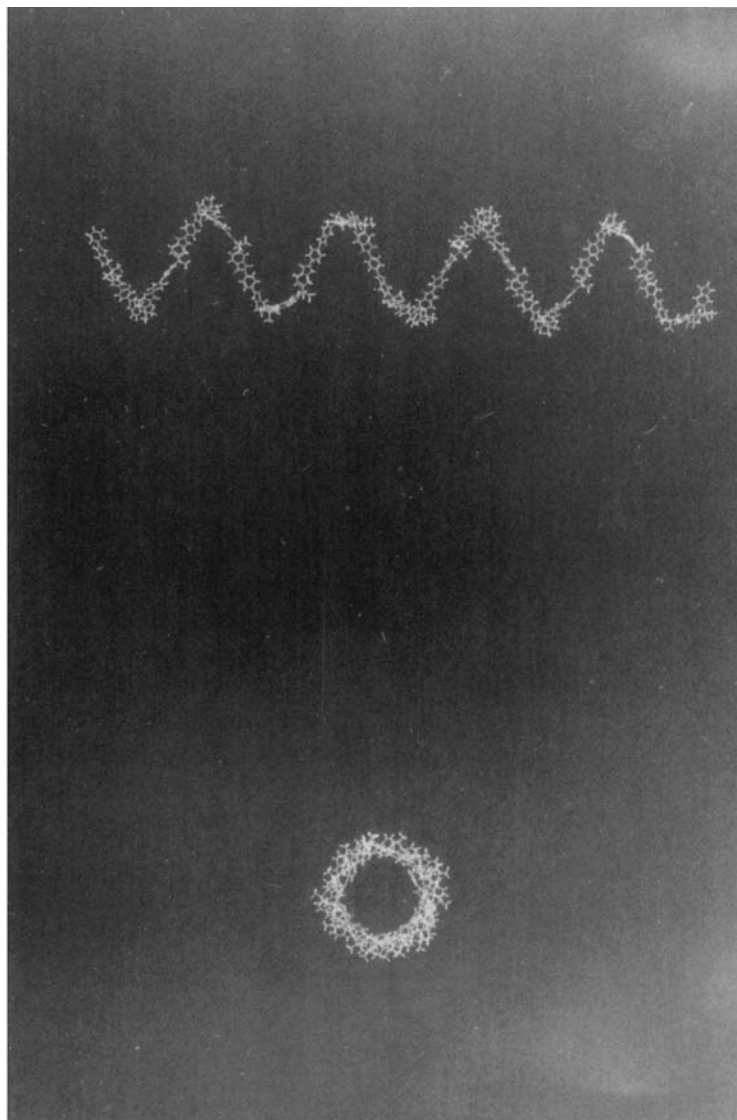


Figure 8 Steric structure of 6FDA-*p*-PDA polyimide with 942 atoms simulated by using computer calculation.

the diffusion of the gas. This suggests that the $-\text{C}(\text{CF}_3)_2-$ group contributes to the increase in the free volume of the polymer. The polymer structures are investigated using a computer graphic that is obtained by molecular dynamic calculation.¹¹ 6FDA polyimides show a helix configuration due to bending and twisting of polymer chain at the carbon atom having $-\text{C}(\text{CF}_3)_2-$ substituent group, as shown in Figure 8. On the other hand, polyimides without $-\text{C}(\text{CF}_3)_2-$ group give straight configuration. A helix configuration can be one of the important reasons for high permeability of hexafluoro-substituted polyimides. Packing of the polymer is difficult by helix configuration and also gas molecules cannot easily pass among the polymer chain.

In this way, helix configuration works effectively for both permeability and selectivity.

Since 6FDA-*p*-PDA shows a larger helix than does 6FDA-4,4'-ODA,¹¹ 6FDA-*p*-PDA is supposed to have higher free volume inside of the polymer structure.

The dependence of gas permeability on pressure and temperature by all 6FDA polyimide films obtained from this work has been investigated. Mean permeability coefficients of a number of gases as a function of upstream pressure are illustrated in Figure 9 for 6FDA-*p*-PDA (film D) and in Figure 10 for 6FDA-4,4'-ODA (film A). Almost the same trend appeared at every temperature: Mean permeability coefficients are approximately independent of the

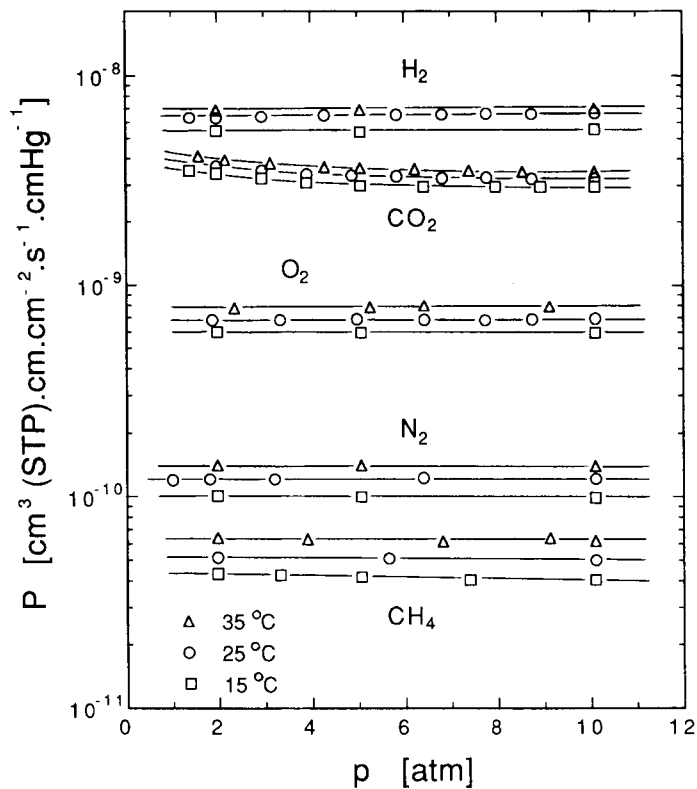


Figure 9 Effect of pressure on mean permeability coefficient of five kinds of gas in 6FDA-*p*-PDA polyimide D film at different temperatures.

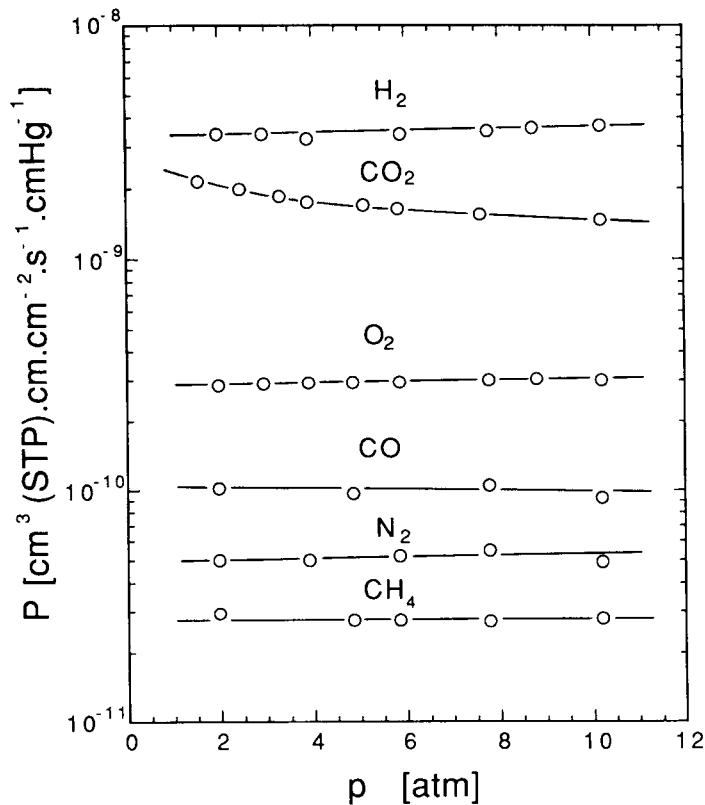


Figure 10 Effect of pressure on mean permeability coefficient of six kinds of gas in 6FDA-4,4'-ODA polyimide A film at 25 °C.

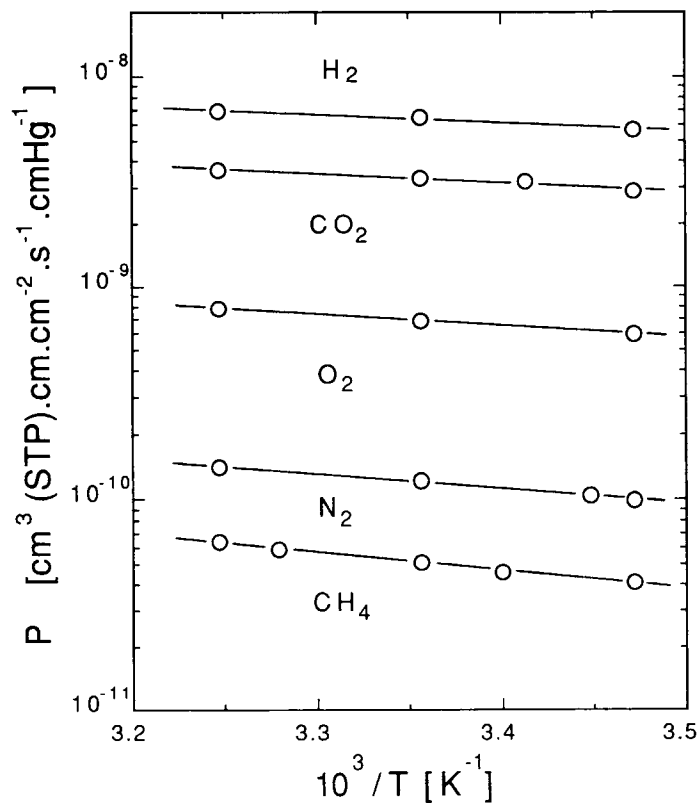


Figure 11 Effect of temperature on mean permeability coefficient of gases in 6FDA-*p*-PDA polyimide D film.

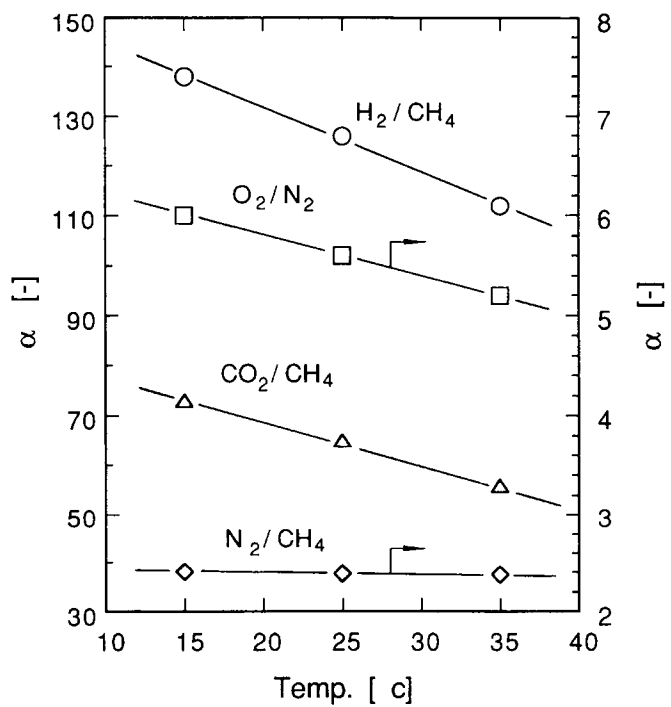


Figure 12 Temperature dependence of ideal separation factor of various gas pairs in 6FDA-*p*-PDA polyimide D film.

Table II Permeation Capabilities of the 6FDA-*p*-PDA Asymmetric Membranes

Gas	H ₂	CO ₂	O ₂	CO	N ₂	CH ₄
$J_i \times 10^3$	214	112	20.2	6.14	4.38	1.98
J_i/J_{CH_4}	108	56.6	10.2	3.1	2.21	1

J_i is at 1 atm and at 25°C in [m³ (STP)/m² h atm].

gas pressure except CO₂, similar to those observed by Stern et al.²

Permeabilities of the 6FDA polyimides to different gases decrease in the order $P_{H_2} > P_{CO_2} > P_{O_2} > P_{N_2} > P_{CH_4}$; this is also the order of increasing "kinetic" diameters¹² of the penetrant molecules. This shows that diffusion selectivity plays an important role for 6FDA polyimides.

Kinetic diameters in Å are

$$H_2 = 2.89 < CO_2 = 3.30 < O_2 = 3.46 \\ < N_2 = 3.64 < CH_4 = 3.80$$

The relationship between mean permeability coefficients of various gases through 6FDA-*p*-PDA (film D) and temperature are shown in Figure 11 at 5 atm. It is clear from Figure 11 that the temperature dependence of the mean permeability coefficients of 6FDA polyimide can be described by the Arrhenius equation since the difference of mean solubility coefficients of 6FDA polyimides is small in the range of temperature covered. Similar results are obtained in other aromatic polyimides.¹³ The effect of temperature on the ideal separation factor α_{ij} for various gas pairs is indicated in Figure 12. With increasing

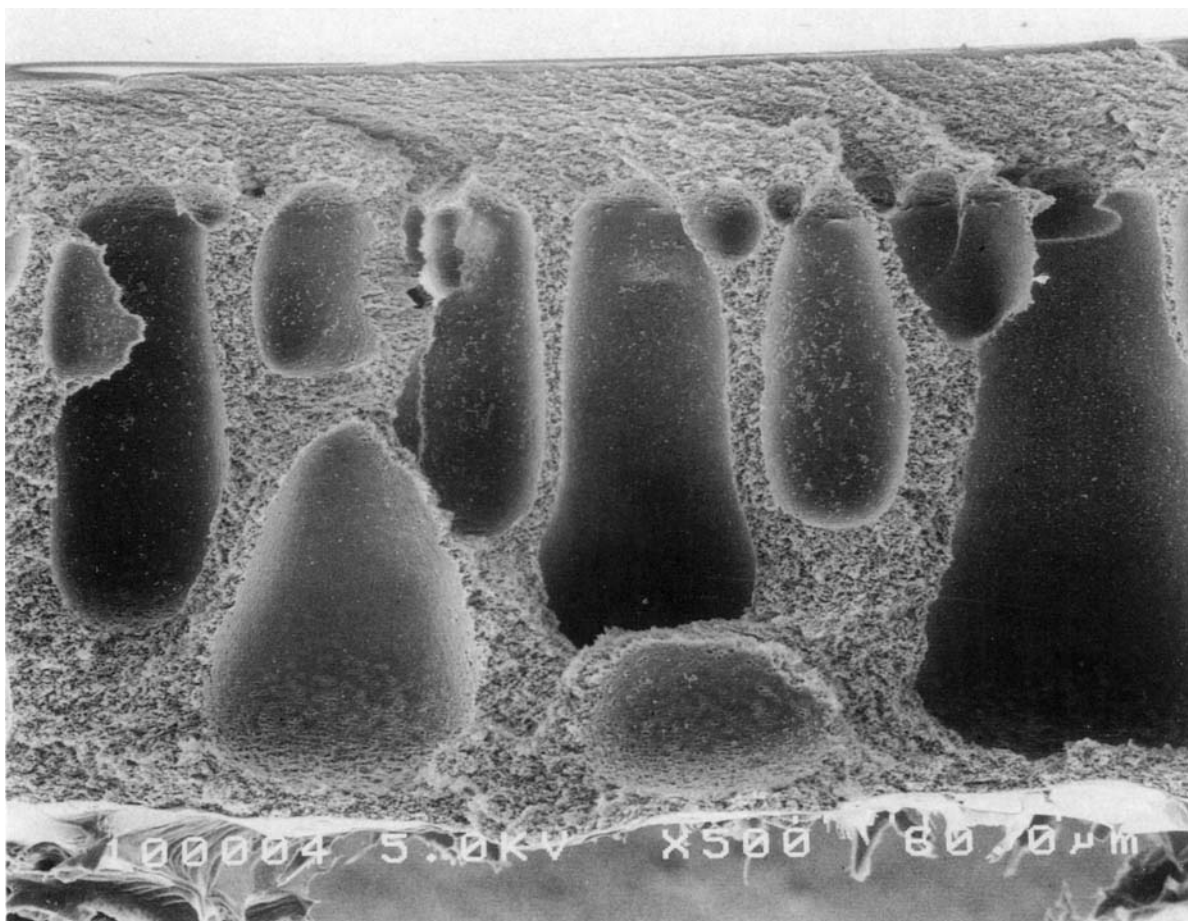


Figure 13 Scanning electron micrograph of the cross section of the 6FDA-*p*-PDA asymmetric membrane stripped from nonwoven cloth.

temperature from 15 to 35°C, except for α_{N_2/CH_4} , the ideal separation factor of each gas pair markedly decreased; α_{CO_2/CH_4} decreased by about 21%.

In the present work, 6FDA polyimide asymmetric membrane composed of a thin skin layer and a thick porous support layer was made on polyester nonwoven cloth by the solution-casting method. The permeation flux of six kinds of gases and the ideal separation factor for methane in 6FDA-*p*-PDA polyimide are listed in Table II as a typical example.

A cross section of 6FDA-*p*-PDA asymmetric membranes are shown in Figures 13–15 using SEM. Figure 13 shows a cross section of the asymmetric membrane stripped from polyester nonwoven cloth; large finger voids are observed in the spongy support area. Magnification of the area with the skin layer is shown in Figure 14; the difference between the dense skin layer and the sponge support layer is

clearly observed. Skin layer thickness evaluated from SEM pictures is around 1.0–2.0 μm , as shown in Figure 15. On the other hand, the thickness of skin layer can be estimated by using a permeation rate of gases through homogeneous film and asymmetric membranes.^{13–15} By using the data from Figure 9 and Table II, the thickness of the skin layer is estimated at around 0.76–1.0 μm . This difference comes from the nonuniform structure of the skin layer, and the actual thickness of the skin layer is not observed.

Capability deterioration of the asymmetric membrane as a function of time was studied by continuous measurement of the permeation rate for 19 days. As shown in Figure 16, there does not appear a remarkable degradation of selectivity within this experiment.

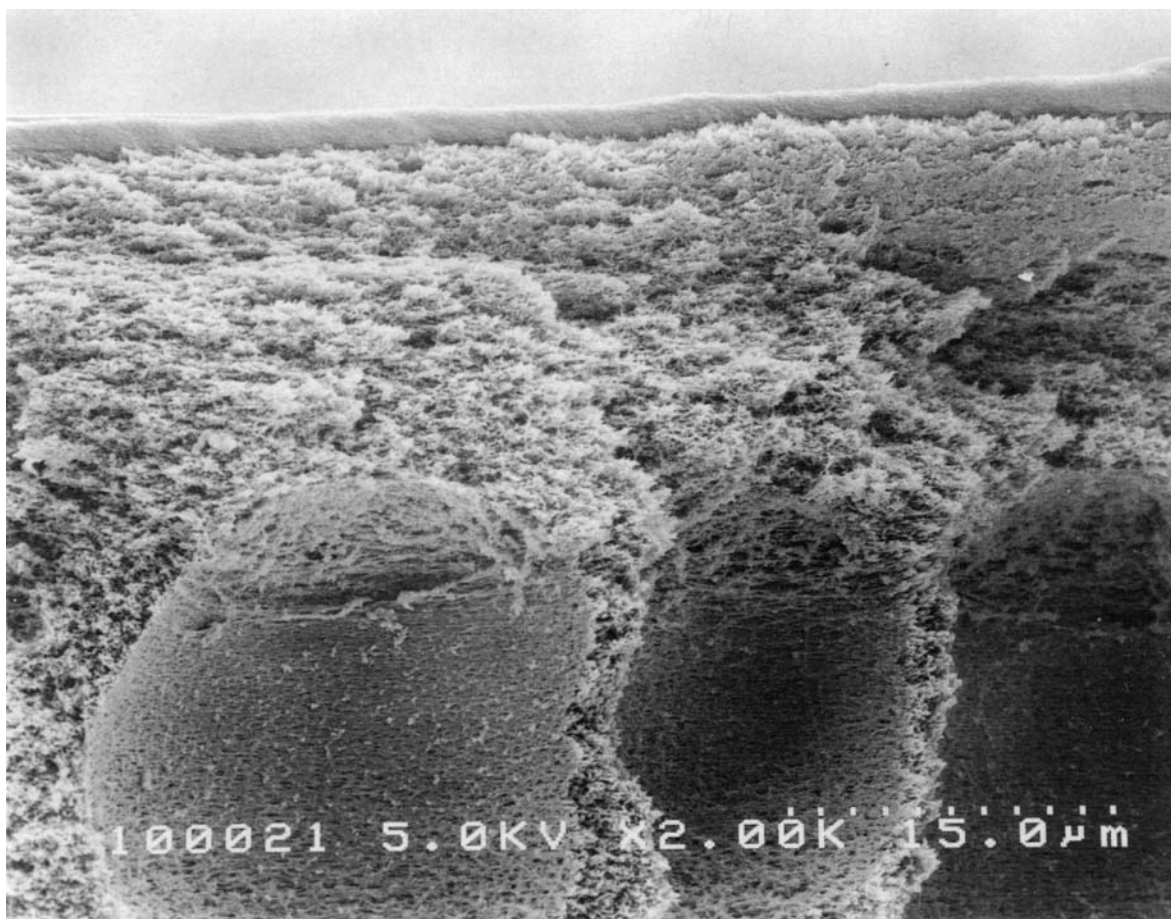


Figure 14 Scanning electron micrograph of the local cross section of the 6FDA-*p*-PDA asymmetric membrane.



Figure 15 Local magnification of the cross section near the skin layer of the 6FDA-*p*-PDA asymmetric membrane.

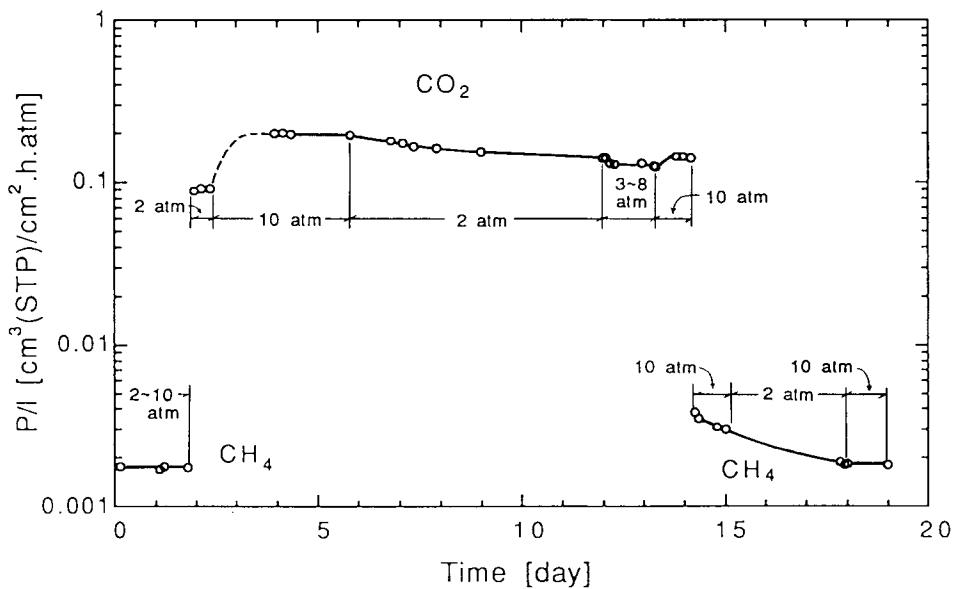


Figure 16 Permeation rate of CO_2 and CH_4 in the same 6FDA-*p*-PDA asymmetric membrane as a function of permeation time at 25°C and at different pressures.

CONCLUSIONS

The main results in the present work are summarized as follows:

The synthesis condition is important to obtain high-selectivity and high-permeability membranes. The chemical imidization method with an optimum condition and higher purity monomer gives higher-capability 6FDA polyimide membranes.

6FDA polyimides exhibit both a higher gas selectivity and permeability than do the presently available polymers. One of the reasons is the helix configuration of 6FDA polyimides, which contributes the increase in free volume of the polymer and controls the diffusivity of the penetrant gas molecules.

Although CO₂ permeability decreased with increasing pressure in the low-pressure range, other gas permeabilities show practically no pressure dependence. On the other hand, gas permeabilities increase with increasing temperature. The ideal separation factor α_{ij} decreases with increasing temperature, except for α_{N_2/CH_4} .

Asymmetric membranes with high gas permeation flux and high selectivity were prepared. Capability deterioration due to a plasticization effect of carbon dioxide on this membrane was not observed in a continuous 19 days measurement.

Much better composite membrane of 6FDA polyimide can be prepared with improved membrane formation technology.

REFERENCES

1. T. H. Kim, W. J. Koros, G. R. Husk, and K. C. O'Brien, *J. Membr. Sci.*, **37**, 45 (1988).
2. S. A. Stern, Y. Mi, and H. Yamamoto, *J. Polym. Sci. Part B Polym. Phys. Ed.*, **27**, 1887 (1989).
3. T. H. Kim, W. J. Koros, and G. R. Husk, *J. Membr. Sci.*, **46**, 43 (1989).
4. M. R. Coleman and W. J. Koros, *J. Membr. Sci.*, **50**, 285 (1990).
5. K. Tanaka, H. Kita, and K. Okamoto, *Senigakkaisi*, **46**, 541 (1990).
6. Y. Kobayashi and T. Kasai, *Proceed. ICOM'90*, 1407 (1990).
7. E. Smit, H. A. Teunis, R. M. Meertens, K. P. M. Kamps, B. A. M. Venhoven, M. H. V. Mulder, and C. A. Smolders, *Proceed. ICOM'90*, 786 (1990).
8. K. Toi, H. Suzuki, T. Ito, I. Ikemoto, and T. Kasai, *Polym. Prepr. Jpn.*, **40**, 3401 (1991).
9. H. Kita, K. Tanaka, and K. Okamoto, *Polym. Prepr. Jpn.*, **40**, 3404 (1991).
10. T. Hirose, Y. Mi, S. A. Stern, and A. K. St. Clair, *J. Polym. Sci. Part B Polym. Phys. Ed.*, **29**, 341 (1991).
11. K. Matsumoto, Y. Minamizaki, and P. Xu, *Maku (MEMBRANE)*, in press.
12. A. R. Berens and H. B. Hopfenberg, *J. Membr. Sci.*, **10**, 290 (1982).
13. E. Sada, H. Kumazawa, P. Xu, and M. Nishigaki, *J. Membr. Sci.*, **37**, 165 (1988).
14. E. Sada, H. Kumazawa, and P. Xu, *J. Appl. Polym. Sci.*, **35**, 1947 (1988).
15. E. Sada, H. Kumazawa, Y. Yoshio, S.-T. Wang, and P. Xu, *J. Polym. Sci. Part B Polym. Phys. Ed.*, **26**, 1035 (1988).

Received March 20, 1992

Accepted May 12, 1992